Available online at www.sciencedirect.com
SCIENCE DIRECT®
Journal of Molecular Catalysis A: Chemical 223 (2004) 321–328
JOURNAL OF MOLECULAR CATALYSIS A: CHEMICAL
www.elsevier.com/locate/molcata

Cerium fluoride supported V_2O_5 catalysts: physico-chemical characterization and 3-picoline ammoxidation activity

K.V. Narayana[b], B. David Raju[a], S. Khaja Masthan[a], V. Venkat Rao[a], P. Kanta Rao[a], A. Martin[b,*]

[a] *Catalysis and Physical Chemistry Division, Indian Institute of Chemical Technology, Hyderabad 500007, India*
[b] *Institute fur Angewandte Chemie, Berlin Adlershof e.V., Richard-Willstatter-Str. 12, D-12489 Berlin, Germany*

Received 12 March 2003; received in revised form 19 January 2004; accepted 1 February 2004
Available online 18 September 2004

Abstract

V_2O_5/CeF_3 catalysts with 2.4–15.2 wt.% of V_2O_5 were prepared by wet impregnation method. The catalysts were characterized by BET surface area and pore size distribution, powder X-ray diffraction and FT-IR. It was found that the formation of Cerium Vanadate ($CeVO_4$) occurs during the stages of the catalyst preparation. The X-ray diffraction studies of the catalysts revealed the presence of crystalline $CeVO_4$ phase. The lines due to $CeVO_4$ phase were found to increase in intensity with the increase in amount (wt.%) of V_2O_5 in the catalysts. The FT-IR investigation also showed the formation of $CeVO_4$ phase with increasing loadings of V_2O_5. The shift of pore-size distribution to lower pore range and increased pore volume confirmed the formation of $CeVO_4$ structure in the catalysts. The catalytic activity for the ammoxidation of 3-picoline to nicotinonitrile on V_2O_5/CeF_3 catalysts as a function of V_2O_5 loading on CeF_3 has been studied. The continuous increase of $CeVO_4$ with V_2O_5 loadings is responsible for the higher ammoxidation activity of the V_2O_5/CeF_3 catalysts.
© 2004 Elsevier B.V. All rights reserved.

Keywords: V_2O_5/CeF_3 catalysts; $CeVO_4$; Ammoxidation; 3-Picoline; Nicotinonitrile.

1. Introduction

It is well known that the TiO_2, Al_2O_3, SiO_2, SnO_2 and ZrO_2 are conventional supports for the V_2O_5 catalysts for oxidation and ammoxidation reactions such as selective oxidation of *o*-xylene to phthalic anhydride [1,2], ammoxidation of propane to acrylonitrile [3–5], methyl benzenes to corresponding benzonitriles [6,7], methyl pyrazine to cyano pyrazines [8] and methyl pyridines to corresponding cyano pyridines [9–11]. Due to stringent environmental legislations more active and selective catalysts are being sought. Hence, deep insight in to selection of compatible catalysts and supports is one of the research goals of the topic. As on today, V_2O_5-based catalysts are of prime importance in the oxidation as well as ammoxidation of light paraffins, olefins and aromatics as shown recently by Grasselli in a review on advances and future trends in selective oxidation and ammoxidation catalysis [12]. Zhang et al. [13] have prepared and used CeF_3 supported rare earth oxide catalysts, CeO_2/CeF_3, $La_2O_3/4CeF_3$ and $Sm_2O_3/4CeF_3$ for oxidative dehydrogenation of propane. Zhang et al. [14] have also prepared a highly active multivalent anion modified complex catalyst, Y_2O_3 + CeF_3 and evaluated for selective oxidative dehydrogenation of isobutane to isobutene. Sichkar et al. [15] have found that CeF_3 is a better support for Pd in hydrogenation of 1-heptene than NaF, CaF_2, MgF_2, BaF_2 and AlF_3, etc. CeF_3 was also used as a support for preparing highly dispersed Au catalysts with Au particle size <10 nm for oxidation reactions [16]. As it is evident from the literature that the fluoride supported V_2O_5 catalysts are active and selective for the ammoxidation reactions [17–20], CeF_3 has judicially been selected as the support for the V_2O_5 catalysts for the ammoxidation of 3-picoline.

* Corresponding author. Tel.: +49 30 6392 4306; fax: +49 30 6392 4350.
E-mail address: a.martin@aca-berlin.de (A. Martin).

1381-1169/$ – see front matter © 2004 Elsevier B.V. All rights reserved.
doi:10.1016/j.molcata.2004.02.033

Results of our recent study [9] on the CeO_2 as a catalyst for ammoxidation of picolines and the documented literature [13–20] have prompted us to explore whether CeF_3 can be used as a novel support for vanadia catalysts and further investigate their physico-chemical characteristics and ammoxidation activity for 3-picoline.

In the present study, we communicate the preparation of cerium fluoride supported V_2O_5 catalysts and their physico-chemical characterization in support of $CeVO_4$ formation. The catalytic performance of these catalysts for the vapor phase ammoxidation of 3-picoline to nicotinonitrile has also been described as a preliminary investigation.

2. Experimental

2.1. Catalyst preparation

CeF_3 supported vanadia catalysts containing 2.4–15.2 wt.% V_2O_5 content were prepared by wet impregnation technique using required amounts of ammonium metavanadate (Aldrich) dissolved in oxalic acid solution to impregnate CeF_3. The excess water in the impregnated samples was evaporated to dryness on a water bath, oven dried at 120 °C for 16 h and finally calcined at 450 °C for 6 h.

2.2. Atomic absorption spectrometer

The vanadium contents in the catalysts were estimated by using Perkin-Elmer-2380 Atomic Absorption Spectrometer. The catalyst samples were decomposed in aquaregia and the resultant solution was diluted with double distilled water to known concentrations.

2.3. Pore size distribution measurements

Measurements for specific surface areas and pore size distributions of the catalysts were made using Quantachrome, Autoscan-92 Porosimeter (U.S.A) by taking 300–500 mg of sample. Accurate data acquisition was made with on line computer analysis.

2.4. Powder X-ray diffraction studies

X-ray diffraction patterns of V_2O_5/CeF_3 catalysts were recorded on a Philips PW-1140 X-ray diffractometer using Ni filtered Cu Kα radiation. In this technique a fixed wave length is chosen for the incident radiation and Bragg peaks are measured by observing the intensity of the scattered radiation as a function of scattering angle of 2θ, the inter planar distances or d-spacings are calculated and compared the data with the available ASTM cards to identify the phase composition in the catalysts.

2.5. FT-IR studies

FT-IR spectra of the catalysts were recorded on Nicolet-740 FT-IR spectrometer. Self-supporting discs of the catalysts were prepared with KBr by applying pressure. These discs were used for recording FT-IR spectra.

2.6. BET-analysis

BET surface areas of the catalysts were estimated using an all glass high vacuum system capable of attaining pressures as low as 10^{-6} Torr by the adsorption of N_2 at liquid nitrogen temperature (−196 °C).

2.7. Catalytic activity tests

3-Picoline ammoxidation runs were carried out in a fixed bed micro catalytic reactor. The reactor was built in-house with pyrex glass and heated in an electric furnace with temperatures ranging from 300 to 410 °C. The reaction was performed at an atmospheric pressure with a molar ratio of 3-picoline: H_2O:NH_3:air = 1:13:6:44, at WHSV of 5.33 gmol/h. The organic feed (3-picoline) mixed with water (1:13 molar ratio) was injected by means of an infusion pump. About 2 g of catalyst was loaded in the reactor and then reduced in H_2 flow at 450 °C for 2 h. Steady-state conditions were obtained after a few hours of reaction. An activity run was made without catalyst using diluents (glass beads), and found that the 3-picoline has not been converted, ruling out the surface volume reaction. The product stream was collected and analyzed by gas chromatograph, equipped with FID module with a column of 10% OV-17 on chromosorb W. The products were also analyzed and confirmed by GC-MS.

3. Results and discussion

3.1. Catalyst preparation and characterisation

The formation of $CeVO_4$ compound was found in the calcined catalysts due to the interaction of V_2O_5 with the cerium atoms of CeF_3 support during the course of the calcination. Several authors have prepared this compound by solid-state reaction of CeO_2 and V_2O_5 in air [21–23]. It has also been reported that $CeVO_4$ was obtained by the reaction between Ce^{3+} salts or its oxide and V_2O_5 under an inert atmosphere because of the instability of Ce^{3+} in air at high temperatures [24,25]. Several studies regarding the oxidation state of cerium in the $CeVO_4$ has been reported unambiguously it is as Ce^{3+} [25–29]. $CeVO_4$ crystallizes in a tetragonal zircon ($ZrSiO_4$) type structure [30] and it is a p-type semiconductor [25,31,32]. The studies of Abi-Aad et al. revealed the Ce^{3+}–V^{4+} segregates formation when treated at 800 °C and their concentration became significant after a reduction treatment under hydrogen flow [33].

Table 1
Variation of surface area and pore volume with V_2O_5 loading on CeF_3 support

Catalyst V_2O_5 (wt.%)[a]	Surface area[b] ($m^2\ g^{-1}$)	Surface area[c] ($m^2\ g^{-1}$)	Pore volume[c] ($cm^3\ g^{-1}$)
2.4	26.0	19.5	0.223
5.4	25.0	17.8	0.307
7.8	23.4	15.8	0.318
10.7	19.3	11.3	0.319
15.2	19.1	12.2	0.293
Pure CeF_3	33.9	29.0	0.410
Pure V_2O_5	6.0	–	–

[a] Estimated by atomic absorption spectrometer.
[b] Surface area by BET method.
[c] Surface area and pore volume by mercury penetration method.

3.2. Catalyst characterization

3.2.1. Surface area and pore size distribution studies

Surface areas estimated by both BET and mercury porosimetric methods are compiled in Table 1. The surface areas estimated by mercury porosimetric method are fewer than that of BET method, which may be due to unestimated micropore surface areas of the catalysts by mercury porosimetric method. The BET surface area of pure CeF_3 is 33.9 $m^2\ g^{-1}$, which has continuously been decreasing with increased V_2O_5 loading, which may be due to blockage of pore mouths. Similar decreasing trend with increase in V_2O_5 loading has also been observed in both the surface area determination methods.

The pore volume distributions of V_2O_5/CeF_3 catalysts are presented in Fig. 1. Pure CeF_3 has a surface area of 33.9 $m^2\ g^{-1}$ and pore volume of 0.41 $cm^3\ g^{-1}$. This material has a narrow pore volume distribution in the pore radius range from 6 nm to 12 nm, the highest pore volume distribution occurring at the dominant pore radius of 8 nm (Fig. 1).

Pore volume distribution curves of the catalyst reveal that V_2O_5 loading has highly pronounced effect on the pore-size distribution of these catalysts. When 2.4–7.8 wt.% V_2O_5 is deposited on CeF_3, the resulting catalysts are observed to exhibit pore volume distribution in the pore radius range form 10 nm to 20 nm, which is entirely different from the pore volume distribution from 6 nm to 12 nm of pure CeF_3. When V_2O_5 loading has been increased to 10.7 wt.%, the pore volume distribution shifts further to the higher pore radius range from 12 nm to 50 nm. When V_2O_5 content of the

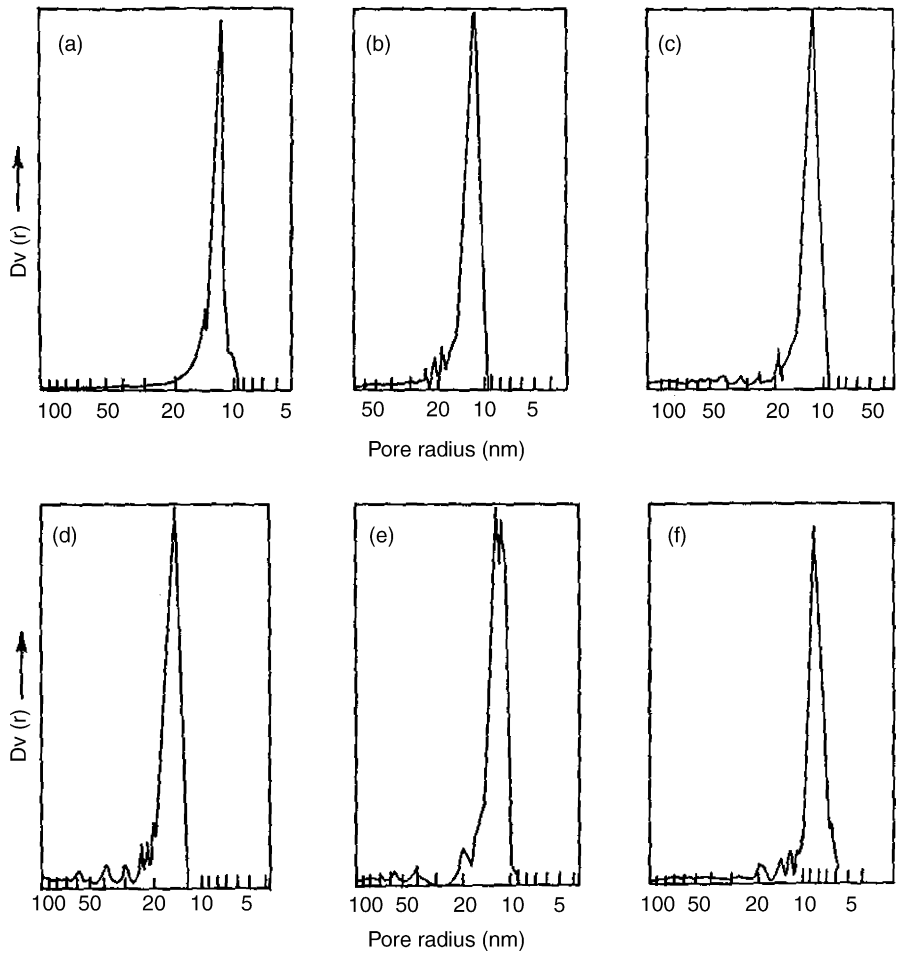

Fig. 1. Pore size distribution curves of V_2O_5/CeF_3 catalysts with different V_2O_5 loadings: (a) 2.4 wt.%, (b) 5.4 wt.%, (c) 7.8 wt.%, (d) 10.7 wt.%, (e) 15.2 wt.%, (f) pure CeF_3.

catalysts is further increased to 15.2 wt.% the pore volume distribution is observed to shift to lower pore radius range, 9–20 nm. The variations in the pore size distributions of the catalysts are reflected in the change of total pore volumes with variations in V_2O_5 loading. Pore volume increases from 0.223 to 0.319 $cm^3\ g^{-1}$ when the V_2O_5 content is increased from 2.4 to 10.7 wt.% due to increase in pore size. When V_2O_5 content is further increased to 15.2 wt.%, the pore volume is reduced to 0.293 $cm^3\ g^{-1}$ due to decrease in pore size. The total surface areas and the total pore volumes of pure CeF_3 and V_2O_5/CeF_3 catalysts are given below in Table 1.

The pore volume distributions of pure CeF_3 and the catalysts clearly reveal that these materials have pore structures in very narrow pore radius range. The contributions of individual pores to the total pore volume and surface area of the catalysts go on decreasing with increase in V_2O_5 loading. V_2O_5/CeF_3 catalysts have exhibited a unimodel distribution of pore sizes.

When V_2O_5 reacts with CeF_3 support to form the compound $CeVO_4$ the bonds of cerium atom to other atoms in CeF_3 are broken and the isolated $CeVO_4$ molecules form tiny crystallites. V_2O_5 might have reacted with and removed the surface layer or even sub-surface layer of cerium atoms and thus bring about an increase in the radii of the pores of the catalyst. This explains the shift of the pore-volume spectra of the catalysts to higher pore radius range till the V_2O_5 loading reaches 10.34 wt.% (Fig. 1). When V_2O_5 loading is increased to 15.2 wt.%, the pore volume distribution shifts to lower pore radius range from 9 nm to 20 nm. This shift of pore-size distribution to lower pore range is occurring due to decrease in the pore size as a result of formation of almost a close packed layer of $CeVO_4$ compound on the walls of cylindrical pores. The dominant pore-size distribution of 15.2 wt.% V_2O_5 catalyst is around 13 nm.

3.2.2. X-ray diffraction

The X-ray diffractograms of fresh and used V_2O_5/CeF_3 catalysts are presented in Figs. 2 and 3 respectively. The X-ray diffractograms of the fresh catalysts contain moderately

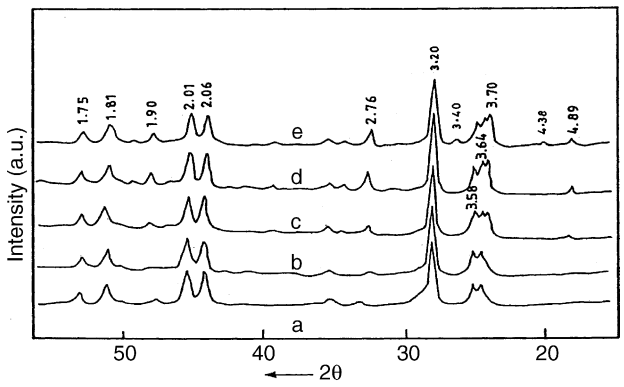

Fig. 2. X-ray diffractograms of V_2O_5/CeF_3 calcined catalysts with different V_2O_5 loadings: (a) 2.4 wt.%, (b) 5.4 wt.%, (c) 7.8 wt.%, (d) 10.7 wt.%, (e) 15.2 wt.%.

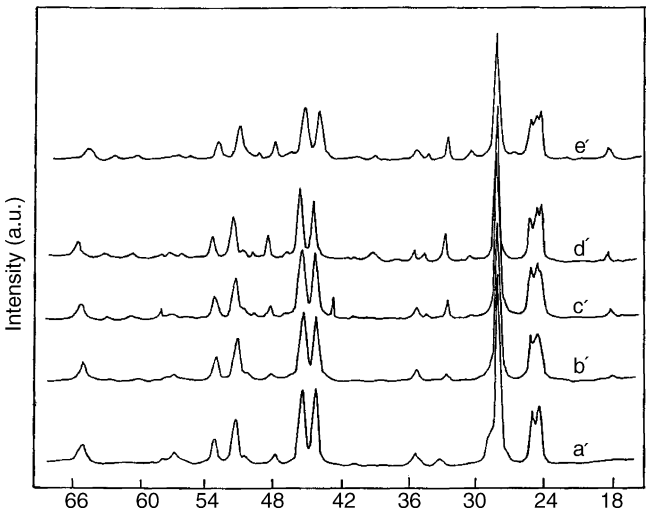

Fig. 3. X-ray diffractograms of V_2O_5/CeF_3 used catalysts with different V_2O_5 loadings: (a^I) 2.4 wt.%, (b^I) 5.4 wt.%, (c^I) 7.8 wt.%, (d^I) 10.7 wt.%, (e^I) 15.2 wt.%.

intense XRD peaks with characteristic *d*-values of 3.20, 2.01, 2.06, 1.81, 3.64, 3.58 and 1.75 Å belonging to the crystal planes (1 1 1), (1 1 3), (3 0 0), (3 0 2), (0 0 2), (1 1 0) and (2 2 1) of CeF_3 support (ASTM card no: 8-45). The intensity of the XRD peaks of CeF_3 support has remained more or less the same with increase in V_2O_5 loading from 2.4 to 15.2 wt.% (Fig. 2). This observation suggests that the surface of the support is not getting covered progressively with increasing V_2O_5 content of the catalysts. The XRD patterns of 2.4 wt.% V_2O_5 catalyst exhibited very weak peaks of the compound, $CeVO_4$ (*d* = 2.76 and 2.57 Å). Very weak XRD peaks with *d*-values of 3.70 and 2.76 Å belonging to crystal planes (2 0 0) and (1 1 2) of $CeVO_4$ phase appear in the catalyst with 5.4 wt.% V_2O_5. The intensity of the XRD peaks of $CeVO_4$ with *d*-values of 3.70, 2.76 and 1.90 Å belonging to crystal planes (2 0 0), (1 1 2) and (3 1 2) (ASTM card No: 12-751) increases gradually with increase in V_2O_5 loading up to 15.2 wt.%. One can visualize an interesting phenomenon occurring on the catalyst surface as a result of interaction of increasing V_2O_5 content with atoms on the surface of CeF_3 support. Deposited V_2O_5 is interacting with the surface of the support generating $CeVO_4$ species which agglomerate to form $CeVO_4$ crystallites and the crystallanity of these species is increasing with increase in V_2O_5 loading. Absence of XRD peaks of any of the oxides of vanadium in the diffractograms of these catalysts upto 10.7 wt % V_2O_5 indicates that entire V_2O_5 has interacted with the cerium atoms of the support to form $CeVO_4$ species. The $CeVO_4$ species might have segregated and crystallized. The exposed CeF_3 support appears to have more open structure with CeF_3 in lower layers being exposed. A shift in the pore size distribution and an increase in pore volume has been observed with increase in V_2O_5 loading of the catalysts, which would lend support to the above explanation. The interaction of vanadia would have occurred not only with surface Ce atoms but also with Ce atoms in the

sub-surface layers of the CeF_3 support. When the V_2O_5 content has been increased to 15.2 wt.% traces of free V_2O_5 have been identified in the X-ray diffractogram of the catalyst.

Careful examination of the results of the X-ray diffraction studies of the used V_2O_5/CeF_3 catalysts would reveal that the surface characteristics of the catalysts have been drastically modified during the course of ammoxidation reaction of 3-picoline (Fig. 2). The most striking feature of the X-ray diffractograms of used catalysts is that they contain the XRD peaks of support which are much more intense than the corresponding peaks in the diffractograms of fresh catalysts (Fig. 3)

The X-ray diffractogram of used 2.4 wt.% V_2O_5/CeF_3 catalyst contains the most intense XRD peaks with *d*-values of 3.20, 2.01, 2.06, 3.64, 3.58, 1.81, 1.75 and 2.55 Å belonging to the crystal planes of (1 1 1), (1 1 3) (3 0 0), (0 0 2), (1 1 0), (3 0 2), (2 2 1), and (1 1 2) of the support CeF_3 (curve-a). When V_2O_5 loading is increased to 5.4 wt.% the intensity of the CeF_3 XRD peak has decreased and a weak XRD peak with a *d*-value of 4.89 Å belonging to $CeVO_4$ phase appears in addition to the XRD peaks of the support (curve-b). When the V_2O_5 loading is increased to 15.2 wt.% the intensity of XRD peaks of the support, CeF_3 is reduced gradually while the intensity of XRD peaks of $CeVO_4$ phase (d = 3.70, 4.89, 2.76 and 1.90 Å) has increased further (curves c–e).

The changes in surface characteristics of the used V_2O_5/CeF_3 catalysts can be attributed to modifications that occur in the surface structure of these catalysts under the severe reaction conditions. These results suggest that under the influence of water vapor, basic molecules and oxygen, the surface $CeVO_4$ species would have diffused on the surface of the catalysts, coalesced and segregated into bigger $CeVO_4$ crystallites. When this has happened these species leave a large surface of the support uncovered and the extent of uncovered surface decreases with increasing V_2O_5 content of the catalysts. This explains the decreasing intensities of the support XRD peaks and the increasing intensities of the peaks of $CeVO_4$ crystallites in the used catalysts (Fig. 3).

Consequently the structural modification and surface reconstruction accompanying catalysis on the support might have occurred to a greater extent in low V_2O_5 catalysts and this accounts for the higher intensities of XRD peaks of low V_2O_5 catalysts (Fig. 2). The observed results of XRD studies of V_2O_5/CeF_3 catalysts seem to be reasonable and valid as the phenomenon of surface modification and reconstruction during adsorption and catalysis is well established [34,35].

3.2.3. FT-IR studies

The FT-IR spectra of the fresh and used V_2O_5/CeF_3 catalysts are given in Figs. 4 and 5 respectively. It is evident that the bands occurring at 3429, 2914, 2837, 2330, 1611–1639 cm^{-1} and 773–801 cm^{-1} are common in the spectra of both fresh and used catalysts. The band at 1724–1731 cm^{-1} is present in the spectra of used catalysts with V_2O_5 loading from 2.4 to 5.4 wt.% and in the spectra of all the fresh catalysts. The band at 3196 cm^{-1} is present

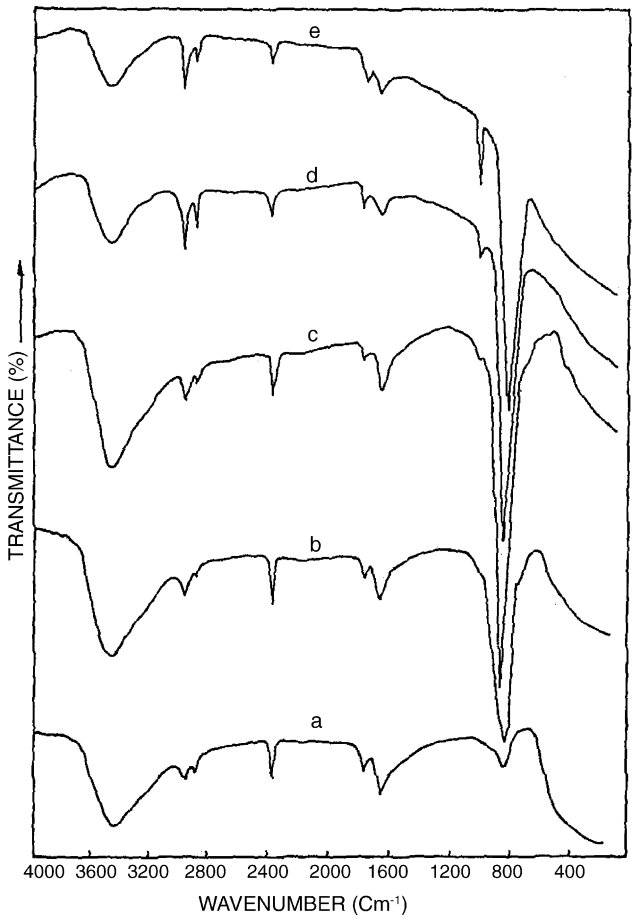

Fig. 4. FT-IR spectra of V_2O_5/CeF_3 calcined catalysts with different V_2O_5 loadings: (a) 2.4 wt.%, (b) 5.4 wt.%, (c) 7.8 wt.%, (d) 10.7 wt.%, (e) 15.2 wt.%.

in the spectra of used catalysts at and above 7.8 wt.% V_2O_5 loading. The band at 1386–1407 cm^{-1} appears in the spectra of all the used catalysts. The band at 1006 cm^{-1} is occurring in the spectra of fresh catalysts at and above 7.8 wt.% V_2O_5 content.

The band at 780–802 cm^{-1} is weak in the spectrum of 2.4 wt.% V_2O_5 catalyst (Figs. 4 and 5). Its intensity has abruptly increased when the V_2O_5 loading is increased to 5.4 wt.% and persists in the spectra of all the catalysts. A band at 780 cm^{-1} is also found in the spectrum of pure CeF_3 (spectrum not shown here). The increase in the intensity of the band at 780–802 cm^{-1} with addition of 5.4 wt.% V_2O_5 may be ascribed to the formation of $CeVO_4$ by the interaction of V_2O_5 with CeF_3. Wachs et al. [36,37] have assigned the laser Raman band at 805 cm^{-1} to the stretching vibrations of V–Ce–O species formed on V_2O_5/CeO_2 catalysts.

The three bands occurring at 3429 cm^{-1}, 2927 cm^{-1} and 2837 cm^{-1} appearing in the spectra of all the catalysts can be attributed to strongly adsorbed water on the surface of CeF_3 support. The spectrum of pure CeF_3 is found to contain highly intense bands at 2927 cm^{-1} and 2837 cm^{-1}. These bands are highly suppressed when 2.4 wt.% V_2O_5 is deposited on the

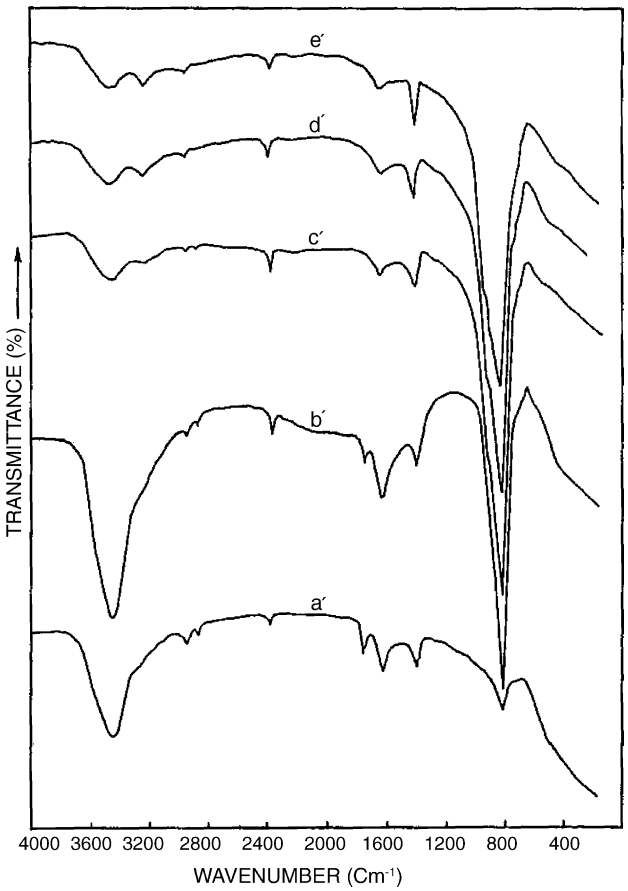

Fig. 5. FT-IR spectra of V_2O_5/CeF_3 used catalysts with different V_2O_5 loadings: (a^I) 2.4 wt.%, (b^I) 5.4 wt.%, (c^I) 7.8 wt.%, (d^I) 10.7 wt.%, (e^I) 15.2 wt.%.

CeF_3 support and exists with very low intensities in the spectra of all the catalysts. The intensity of the broad band at 3429 cm^{-1} and the intensity of the narrow band at 2337 cm^{-1} have increased upto 7.8 wt.% V_2O_5 and decreased above this loading. However, the intensity of the bands at 2927 cm^{-1} and 2837 cm^{-1} has continuously increased with V_2O_5 loading of the fresh (calcined) catalysts (Fig. 4). The band at 1611–1639 cm^{-1} that exists on the surface of all the fresh catalysts may be assigned to deformation vibrations of strongly adsorbed water [38,39]. The band at 1006 cm^{-1} can be attributed to asymmetric stretching vibrations of V=O bonds and the intensity of this peak increases with increase in V_2O_5 loading from 7.8 wt.% to 15.2 wt.%.

The intensity of the band at 3429 cm^{-1} increases when the V_2O_5 loading is increased from 2.4 wt.% to 5.4 wt.% and decreases above this loading in the spectra of used catalysts (Fig. 5) indicating decrease in OH group concentration on the surface of the used catalysts. The intensity of the band at 1618 cm^{-1} decreases with increase in V_2O_5 loading. The band at 1386–1407 cm^{-1} increase in intensity continuously with V_2O_5 loading. This band and the band at 3196 cm^{-1} in the spectra of used catalysts with 7.8, 10.7 and 15.2 wt.% V_2O_5 loading may belong to adsorbed NH_4^+ ions [20]. The narrow band at 2330 cm^{-1} is prominent in the spectra of fresh catalysts (Fig. 4) and become weak in the spectra of used catalyst (Fig. 5).

3.3. Catalytic activity studies

Ammoxidation of 3-picoline over all V_2O_5/CeF_3 catalysts at different temperatures ranging from 300 to 410 °C at atmospheric pressure in the vapor phase at the mole ratio of 3-picoline:H_2O:NH_3:air = 1:13:6:44 (W/F = 5.33 gh/mole) produced mainly nicotinonitrile along with small quantities of pyridine, CO_x and a trace amount of pyridine amide.

Pyridine and CO_x are produced directly from 3-picoline by oxidative demethylation or via nicotinonitrile and pyridine amide, in which nicotinonitrile gets converted in to pyridine amide by acid hydrolysis, hydrolysis of pyridine amide leads to the production of pyridine and CO_x at the applied reaction conditions on the surface of the V_2O_5/CeF_3 catalysts (Scheme 1). In order to find out the major reactant for the formation pyridine and CO_x by-products in the system an experiment was conducted mixing the 3-picoline, nicotinonitrile, pyridine amide and water in accordance with the molar ratios of reaction effluents under similar reaction conditions and observed only a trace amounts of pyridine and CO_x, which clearly indicates that the demethylated products are mainly from 3-picoline by oxidative demethylation. There is a striking balance (1:1 mole ratio) between the formed pyridine and CO_x, which is an indication of CO_x production, is only from the methyl group of 3-picoline, not from the total oxidation of 3-picoline (Scheme 1). Bondareva et al. [8] put similar observation forward in the ammoxidation of 2-methylpyrazine over V–Ti oxide system.

Nicotinonitrile is the ammoxidation product of 3-picoline, in which one molecule of 3-picoline and one molecule of ammonia, and one half dioxygens are consumed for the production of one molecule of nicotinonitrile and three molecules of H_2O, which indicates that the ammoxidation of 3-picoline is a six-electron redox process. It is reported that the ammoxidation of methyl aromatics or methyl heteroaromatics starts from the H-abstraction from the methyl group and forms a methylene-like (benzyl) species, which converts in to benzaldimine (R–CH_2=NH) intermediate either by dehydrogenation of intermediately generated benzylamine (R–CH_2–NH_2 produced from benzyl species) or by dehydration of ammonia condensed-benzaldehyde [6,40]. Busca et al. reported that the nitrile could also be formed from benzaldehyde intermediate by its oxidation to corresponding acid with subsequent acid amide (R–$CONH_2$) formation and dehydration [41].

3.3.1. Influence of V_2O_5 loading on the ammoxidation activity

The influence of V_2O_5 loading on 3-picoline conversion, the yield of nicotinonitrile and the pyridine over V_2O_5/CeF_3 catalysts is depicted in Fig. 6. The conversion and the yield of nicotinonitrile have continuously been increasing with V_2O_5

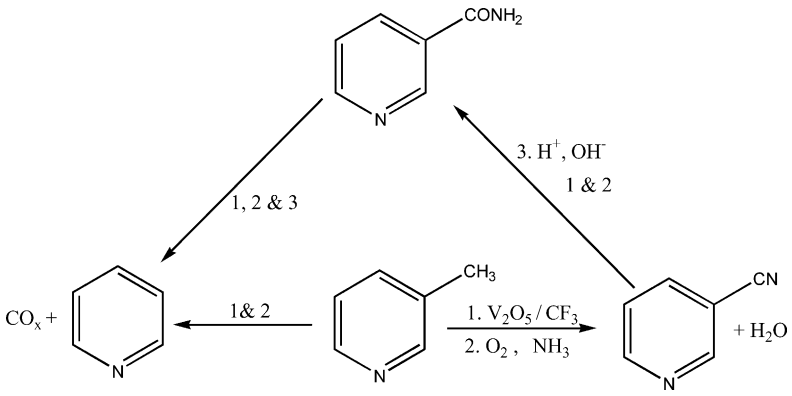

Scheme 1. Reaction pathways of 3-picoline over V_2O_5/CeF_3 catalysts.

loading, whereas the yield of pyridine has shown decreasing trend. The conversion at 2.4 wt.% V_2O_5 loading is 57.9% and it attained a maximum value of 89.18% at 15.2 wt.% V_2O_5 loading. The yield of nicotinonitrile is 37.87% at 2.4 wt.%, which has steadily been increased to 81.92% as the loading of V_2O_5 increased to 15.2 wt.%. The yield of pyridine decreased from 10.13 to 3.63% as the loading of V_2O_5 increased from 2.4 to 15.2 wt.%, similar trend has also been observed in the case of CO_x yield.

The increase in the selective ammoxidation activity of the catalysts with increase in V_2O_5 loading can be attributed to the formation of more active phase, $CeVO_4$. X-ray diffraction study of these catalysts has detected the formation of $CeVO_4$ phase in the catalysts (Fig. 2). The intensity of the XRD peaks of $CeVO_4$ phase is found to increase with increase in V_2O_5 loading. These results show that selective ammoxidation of 3-picoline may be occurring to a greater extent on $CeVO_4$ phase.

Pyridine formation is due to demethylation, which normally takes place on the acidic sites of the catalysts; since CeF_3 is a strong Lewis acid its contribution towards dealkylation is inevitable at lower loadings. The progressive coverage of V_2O_5 on the surface of CeF_3 decreased pyridine yields.

The formation of $CeVO_4$ phase modifies the base V_2O_5/CeF_3 composition. The modification in general will have both electronic as well as structural consequences, but in the present case Ce^{3+} species exists leaving V^{5+} species in the $CeVO_4$ phase [25,31]. Hence, isolation of V–O moieties by interposing of $CeVO_4$ phase between V–O–V chains (site isolation at work) may be responsible for the high yields of nicotinonitrile at higher loadings of V_2O_5 on CeF_3 support. Roussel et al. [42] reported that at higher loadings of Fe in the Fe_{1-x} SbV_xO_4 structure, Fe substitutes V^{3+} by creating a vacancy which enhanced the selectivity to acrylonitrile in the ammoxidation of propane by isolating the active vanadia site and they also reported that the Fe^{3+}/Fe^{2+} couple was not directly involved in the reaction mechanism but that Fe intervenes by changing the relative valence state of vanadium and the cationic and anionic assessment in the structure.

3.3.2. *Influence of reaction temperature on the activity over15.2 wt.% V_2O_5/CeF_3 catalyst*

Temperature is found to have highly pronounced effect on 3-picoline conversion and the yield of nicotinonitrile and pyridine (Fig. 7). The increase in selective 3-picoline ammoxidation activity and the increase in pyridine yield with temperature can be ascribed to the increase in the intrinsic activity of the active sites on the $CeVO_4$ phase and the acidic sites on the bare surface of the support, respectively. At 410 °C, the catalyst has shown 84.78% nicotinonitrile and 5.13% pyridine yield respectively at a 3-picoline conversion of 91.3%.

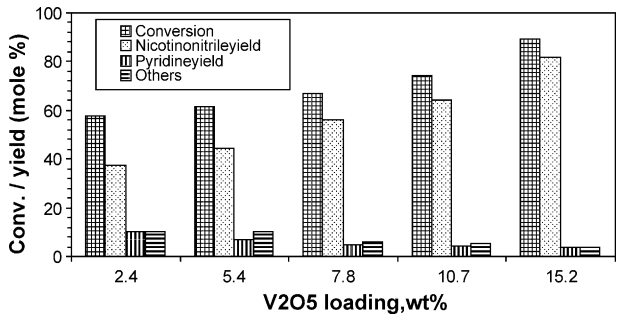

Fig. 6. Influence of V_2O_5 loading on 3-picoline conversion and yields of nicotinonitrile pyridine, CO_x and others.

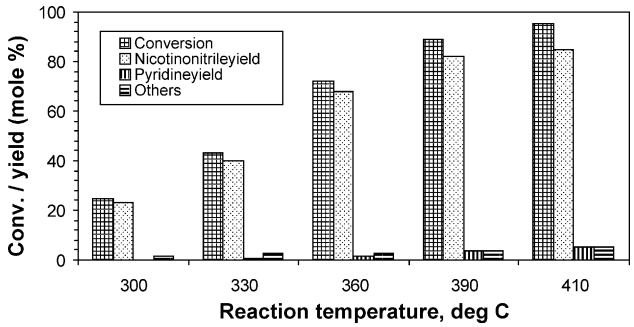

Fig. 7. Effect of reaction temperature on 3-picoline conversion and the yields of nicotinonitrile, pyridine, CO_x and others.

4. Conclusions

It is concluded that the non-conventional CeF_3 supported V_2O_5 catalysts exhibit high conversions and selectivities in the ammoxidation of 3-picoline to nicotinonitrile. This high performance of these catalysts is ascribed to the formation of $CeVO_4$ species during the catalyst preparation. The results of our preliminary investigation gives an impression that highly reactive V_2O_5/CeF_3 or $CeVO_4$-based ammoxidation catalysts can be prepared.

Acknowledgement

K.V. Narayana, one of the authors, expresses his grateful thanks to CSIR, New Delhi for the award of senior research fellowship.

References

[1] M.S. Wainwright, N.R. Foster, Catal. Rev. Sci. Eng. 19 (1979) 211.
[2] V. Nicolov, D. Klissurski, A. Anastasov, Catal. Rev. Sci. Eng. 33 (1991) 1.
[3] R. Catani, G. Centi, F. Trifiro, R. Grasselli, Indus. Eng. Chem. Res. 31 (1992) 107.
[4] T. Ushikubo, K. Oshima, A. Kayou, M. Vaarkamp, M. Hatano, J. Catal. 169 (1997) 394.
[5] T. Shishido, T. Konishi, I. Matsuura, Y. Wang, K. Takaki, K. Takehira, Catal. Today 71 (2001) 77.
[6] A. Martin, B. Lucke, Catal. Today 57 (2000) 61.
[7] R.G. Rizayev, E.A. Mamendov, V.P. Vislovski, V.E. Sheinin, Appl. Catal. A 83 (1992) 103.
[8] V.M. Bondareva, T.V. Andrushkevich, O.B. Lapina, Catal. Today (2000) 173.
[9] P. Kanta Rao, K.S. Rama Rao, S. Khaja Masthan, K.V. Narayana, T. Rajiah, V. Venkat Rao, Appl. Catal. A 163 (1997) 123.
[10] K.V. Narayana, A. Venugopal, K.S. Rama Rao, V. Venkat Rao, S. Khaja Masthan, P. Kanta Rao, Appl. Catal. A 150 (1997) 269.
[11] K.V. Narayana, A. Venugopal, K.S. Rama Rao, S. Khaja Masthan, V. Venkat Rao, P. Kanta Rao, Appl. Catal. A 167 (1998) 11.
[12] R.K. Grasselli, Catal. Today 49 (1999) 141.
[13] W. Zhang, H. Wan, Q. Cai, Gaodeng Xuexio Huaxue Xuebao, 14 (1993) 566 (Ch). CA: 120: 7956w.
[14] W. Zhang, D. Tang, X. Zhou, H. Wan, K.R. Tsai, J. Chem. Soc., Chem. Commun. (1994) 771.
[15] E.V. Sichkar, Yu.M. Bondarev, L.F. Komolova, V.V. Nikitin, Yu.S. Mardashev, Zh. Fiz. Khim. 59 (1985) 2056 (Russ.).
[16] G.D. Kazakova, L.F. Komolova, I.V. Razumovskaya, Yu.S. Mardashev, Zh. Fiz. Khim. 57 (1983) 243 (Russ.).
[17] K.V. Narayana, S. Khaja Masthan, V. Venkat Rao, B. David Raju, P. Kanta Rao, Catal. Commun. 3 (2002) 173.
[18] K.V. Narayana, B. David Raju, S. Khaja Masthan, V. Venkat Rao, P. Kanta Rao, Catal. Lett. 84 (2002) 27.
[19] J. Haber, J. Stoch, M. Wojciechowska, Surf. Interf. Anal. 15 (1990) 711.
[20] J. Haber, M. Wojciechowska, Catal. Lett. 10 (1991) 271.
[21] J.A. Dumesic, H. Topsoe, S. Khammouma, M. Boudart, J. Catal. 37 (1975) 503.
[22] G.C. Bond, Acc. Chem. Res. 26 (1993) 490.
[23] J.M. Jehng, G. Deo, B.M. Weckhyusen, I.E. Wachs, J. Mol. Catal. A 110 (1996) 41.
[24] I.H. Brixner, E. Abramson, J. Electrochem. Soc. 112 (1965) 70.
[25] A. Watanabe, J. Solid State Chem. 153 (2000) 174.
[26] F. Le Normand, J.E. Fallah, L. Hilaire, P. Legare, A. Kotani, J.C. Parlebas, Solid State Commun. 71 (1989) 885.
[27] A. Kotani, T. Jo, J.C. Parlebas, Adv. Phys. 115 (1988) 16.
[28] J.Z. Shyu, K. Otto, W.L.H. Watkins, G. Graham, R.K. Belitz, H.S. Gandhi, J. Catal. 114 (1988) 23.
[29] R. Cousin, M. Dourdin, E. Abi-Aad, D. Courcot, S. Capelle, M. Guelton, A. Aboukais, J. Chem. Soc., Faraday Trans. 93 (1997) 3863.
[30] N.S. Rao, O.G. Palanna, Bull. Mater. Sci 18 (1995) 593.
[31] K. Gaur, H.B. Lal, J. Mater. Sci 20 (1985) 3167.
[32] T. Hirata, A. Watanabe, J. Solid State Chem. 158 (2001) 254.
[33] E. Abi-Aad, A. Bennani, J.P. Bonnelle, A. Aboukais, J. Chem. Soc., Faraday Trans. 91 (1995) 99.
[34] W.O. Mulligan, I.W. Vernon, J. Phys. Chem. 56 (1952) 145.
[35] M. Yoshimura, T. Sata, Bull. Chem. Soc. Jpn. 42 (1969) 3195.
[36] H. Brusset, F. Madule-Aubry, B. Blanck, J.P. Glaziou, J.P. Laude, Can. J. Chem. 49 (1971) 3700.
[37] I.E. Wachs, F.D. Hardcastle, S.S. Chan, Spectroscopy 1 (1986) 30.
[38] G.C. Bond, A.J. Sarkani, G.D. Parfitt, J. Catal. 57 (1979) 476.
[39] K. Nakamoto, Infrared Spectra of Inorganic and Coordination Compounds, Wiley, New York, London, 1963.
[40] G. Busca, ACS Symp. Ser. 523 (1993) 168.
[41] F. Cavani, G. Centi, F. Trifiro, La Chemica and L' Industria. 74 (1992) 182.
[42] H. Roussel, B. Mehlomakulu, F. Belhadj, E. van Steen, J.M.M. Millet, J. Catal. 205 (2002) 97.